RANA 02-29
October 2002

Subgridding in FDTD

by

V. Nefedov
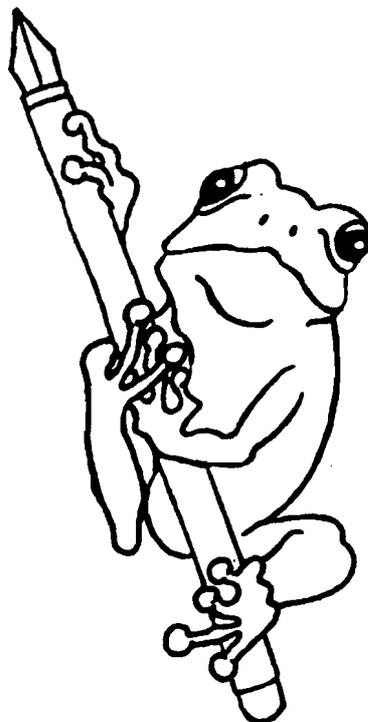
Subgridding in FDTD

V. Nefedov

Introduction

Finite-Difference Time-Domain (FDTD) method, originally proposed by Kane Yee in [18], proved to be a simple and efficient tool in solving Maxwell equations. There are however two major drawbacks to a classical FDTD method.

The first one is related to a situation when we have a two-scale problem. This two-scale situation can be caused by a presence of e.g. scatterer which is much smaller than the size of the problem. To resolve such a problem within a classical FDTD approach we would need to refine the computational domain globally, which would lead to a considerable increase in memory requirements. Since the FDTD is explicit, the stability conditions bounds the time step, thus adding the slower convergence to the memory problems.

The second drawback of classical FDTD is its inefficiency with respect to curved boundaries. Indeed, FDTD was formulated on tensor-product grids only and the only way to interpolated a curved object is by staircase approximation.

In this survey we consider a possible remedy for these drawbacks of FDTD algorithms. The idea is to treat a source of inhomogeneity, whether it is a small in size detail or a curved object, separately, that is to solve the problem in the whole domain on a coarse grid first, then solve the subproblem on a finer grid (or a grid formulated in curvilinear coordinates) and combine the results. This technique is called subgridding and is extensively used for various problems.

The first paper on subgridding for FDTD was published in 1981. Through the last 20 years only about 20 papers followed the original publication. Below we list most of them in chronological order

1981

1. R. Holland and L. Simpson. Finite difference analysis of emp coupling to thin struts and wires.

1

2. K. S. Kunz and L. Simpson. A technique for increasing the resolution of finite-difference solution of the Maxwell equation.

1990

3. Ihn S. Kim and Wolfgang J. R. Hoefer. A local mesh refinement algorithm for the time domain–finite difference method using maxwell's curl equations.

1991

4. Svetlana S. Zivanovic, Kane S. Yee, and Kenneth K. Mei. A subgridding method for the time-domain finite-difference method to solve maxwell's equations.

1992 5. Deane T. Prescott and N. V. Shuley. A method for incorporating different sized cells int the finite-difference time-domain analysis technique.

6. Kane S. Yee, Jei Shuan Chen, and Albert H. Chang. Conformal finite-difference time-domain (FDTD) with overlapping grids.

1996

7. P. Thoma and T. Weiland. A consistent subgridding scheme for the finite difference time domain method.

1997

8. Michael W. Chevalier, Raymond J. Luebbers, and Vaughn P. Cable. FDTD local grid with material traverse.

9. Michal Okoniewski, Ewa Okoniewska, and Maria A. Stuchly. Three-dimensional subgridding algorithm for FDTD.

10. Mikel J. White, Magdy F. Iskander, and Zhenlong Huang. Development of a multigrid FDTD code for three-dimensional applications.

1998 11. T. O. Körner and W. Fichtner. Grid interpolation at material boundaries in finite-difference time-domain methods.

1999

12. S. Chaillou, J. Wiart, and W. Tabbara. A subgridding scheme based on mesh nesting for the FDTD method.

2001

13. Stavros V. Georgakopoulos, Rosemary A. Renaut, Constantine A. Balanis, and Craig R. Birtcher. A hybrid fourth-order FDTD utilizing a second-order FDTD subgrid.

14. Bing-Zhong Wang, Yingjun Wang, Wenhua Yu, and Raj Mittra. A hybrid 2-D ADI-FDTD subgridding scheme for modeling on-chip interconnects.

15. Mikel J. White, Zhengqing Yun, and Magdy F. Iskander. A new 3-D FDTD multigrid technique with dielectric traverse capabilities.

16. Baixin Zhou and Sicong Wang. A hybrid coordinate scheme for enchancing the finite-difference time-domain method.

2002

17. Shumin Wang, Fernando L. Teixeira, Robert Lee, and Jin-Fa Lee. Optimization of subgridding schemes for FDTD.

To keep the story as transparent as possible we decided to restrict our attention to three major topics. First, subgridding when both grids are in cartesian coordinates and the local grid is finer than the global. Second, same as the first but with dielectric boundary possibly traversing the coarse-fine grid interface, and last a combination of global cartesian and local curvilinear grids.

1 VSSM, MRA and MGDM

Throughout this paper we consider a set of simplified Maxwell equations

$$\frac{\partial \mathbf{H}}{\partial t} = -\frac{1}{\mu} \nabla \times \mathbf{E}, \tag{1}$$

$$\frac{\partial \mathbf{E}}{\partial t} = \frac{1}{\epsilon} \nabla \times \mathbf{H}, \tag{2}$$

where $\mathbf{H}$ and $\mathbf{E}$ are the magnetic and the electric fields respectively, μ is a magnetic permeability and ϵ is electrical permittivity.

The computational domain is split into a number of cubes. Each of the cubes holds an arrangement of nodes for electric and magnetic fields, see figure 1. Such an arrangement makes discretisation of the maxwell equations (1) and (2) a trivial matter. Note, that beside staggering in space FDTD also exploits staggering in time, that is the magnetic and electric fields is computed at different time levels. Let us illustrate the discretisation scheme using the $x-$component

3
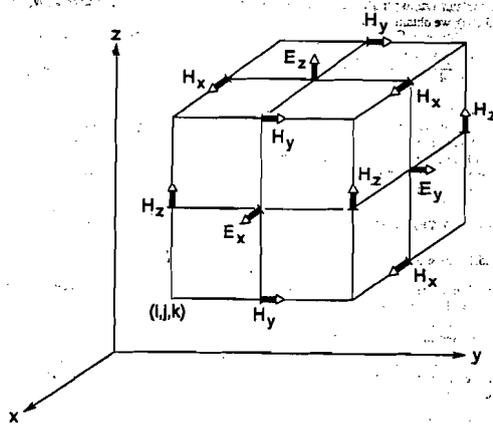
Figure 1: Yee cell

of **E** as an example

$$\frac{E_{x,i+1/2,j+1/2,k}^{n+1} - E_{x,i+1/2,j+1/2,k}^{n}}{\Delta t}$$

$$= \frac{H_{z,i,j+1,k+1/2}^{n+1/2} - H_{z,i,j,k+1/2}^{n+1/2}}{\Delta y} - \frac{H_{y,i,j+1/2,k+1}^{n+1/2} - H_{z,i,j+1/2,k}^{n+1/2}}{\Delta z} \quad (3)$$

Due to explicitness of FDTD algorithm, there exists a restriction on a time step. It relates the time step Δt used in FDTD to a Yee-cell size Δx and the propagation speed of electromagnetic waves $c = 1/\sqrt{(\mu\epsilon)}$

$$\Delta t \le \frac{\Delta x}{c}. \quad (4)$$

Stability condition (4) imposes a rather severe restriction on a size of the time step Δt. Moreover, if our problem is such that the space refinement is needed, then this refinement would inevitably lead to an increase in a number of time steps. To avoid increase in memory and time we can use of of the subgridding algorithms.

In this section we consider several subgridding algorithms exploiting the idea of using the wave equation at the interface between the coarse and the fine grids.

The first algorithm of this group is called Variable Step Size Method (VSSM) and was suggested by Zivanovic, Yee and Mei in [21].

VSSM solves discrete Maxwell equations on a combination of two grids: coarse grid covering the whole computational domain and fine grid covering inhomogeneities.

4

Figure 2: Regions used to calculate fields at the coarse/fine grid interface (from [12])
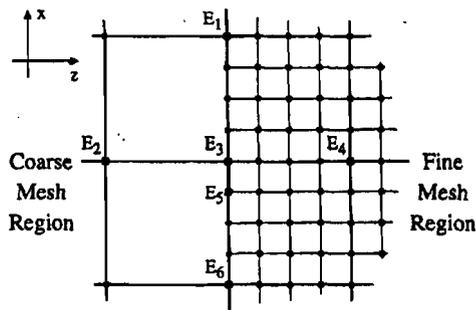
Boundary conditions for the fine grid problem are obtained via an extra equation. To ensure a smooth transition from the coarse to the fine grid a wave equation is solved on the interface

$$\nabla^2 \mathbf{E} - \frac{1}{c^2} \frac{\partial^2 \mathbf{E}}{\partial t^2} = 0. \tag{5}$$

Discretising (5) we obtain an update equation for the electric fields at the interface

$$E^{n+1} = 2E_{i,j,k}^n - E_{i,j,k}^{n-1} + c^2 \Delta t^2$$
$$(\frac{E_{i+1,j,k}^n - 2E_{i,j,k}^n + E_{i-1,j,k}^n}{\Delta^2 x} +$$
$$\frac{E_{i,j+1,k}^n - 2E_{i,j,k}^n + E_{i,j-1,k}^n}{\Delta^2 y} + \tag{6}$$
$$\frac{E_{i,j,k+1}^n - 2E_{i,j,k}^n + E_{i,j,k-1}^n}{\Delta^2 z}).$$

Some of the terms in (6) involve fields evaluated at points external to the fine grid. The use of quadratic approximation was suggested in [21]

The fields in the fine grid are found using FDTD. The tangential electric field is found from the discrete wave equation (6) using the values from both coarse and fine grids. The magnetic field on the interface is calculated using FDTD.

Assume that the fine-grid size is n times smaller than the the coarse-grid size. Then for iteration of FDTD on a coarse grid we need n iterations of FDTD on a fine grid.

A modification to the VSSM algorithm was suggested by Prescott and Shuley in [12]. For simplicity, we illustrate their algorithm – Mesh Refinement Algorithm

5

(MRA) – for TM_y-mode. A mesh reduction factor of 4 will be used as shown in Fig. 2.

We consider the calculation of E_y-components at the interface only, since all other fields are updated via normal FDTD iterations. Assume now $t = t_n$ and all field components corresponding to this time level to be known. We begin by calculating spacial differences D_i, for example at the node 3 we have

$$D_3 = E_2 + E_4 + E_1 + E_6 - 4E_3,$$

where we assume $\Delta x = \Delta y$. Next, the spacial differences are computed for the fine nodes by using quadratic interpolation, e.g.

$$D_5 = D_3 + \frac{D_6 - D_1}{8} + \frac{D_6 + D_1 - 2D_3}{32}.$$

These values can now be used to calculate the field values for the next coarse-grid time step and all of the intermediate fine grid time steps.

At $t = t_n + \Delta t_f$ (f - stands for fine), electric field at the boundary is calculated according to 6)

$$E_5^{n+\Delta t_f} = 2E_5^n - E_5^{n-1} + \frac{c^2 \Delta t_f^2}{\Delta x_f^2} D_5.$$

The difference between the MRA and the VSSM can be seen in the way the second order differences are calculated. In VSSM they are computed from the interpolated values of the electric field on the coarse grid. In MRA coarse grid differences are computed first and than interpolated onto the fine grid. Reversing the order has an advantage of requiring less memory and computational time.

Another modification to the VSSM algorithm was proposed by White, Iskander and Huang, [16]. They mentioned that the procedure of updating the coarse grid fields from the fine grid in VSSM and MRA is not quite clear. Thus, in [16] an original approach was developed. On each common time step the fields are updated in a following fashion

1. the coarse-grid electric fields of the first cell inside the overlapping region are left unchanged;

2. the coarse-grid electric fields of the second cell inside the overlapping region are calculated based on averaging the calculated coarse-grid values calculated from the fine grid;

3. the coarse-grid electric fields of all other cells inside the overlapping region are replaced with the values calculated from the grid.

Figure 3: Comparison between magnitude errors (ϱ_{MAG}) of the electric field as calculated by MGDM and VSSM. The size of the regions were $4 \times 4 \times 4$ fine grid cells (left) and $8 \times 8 \times 8$ fine grid cells (right). Courant number of 0.57 was used in MGDM (from [16]).
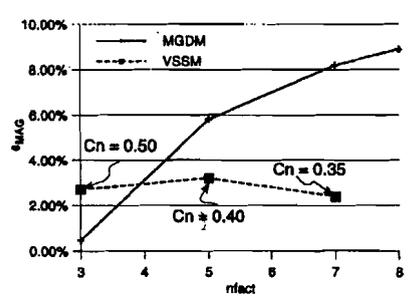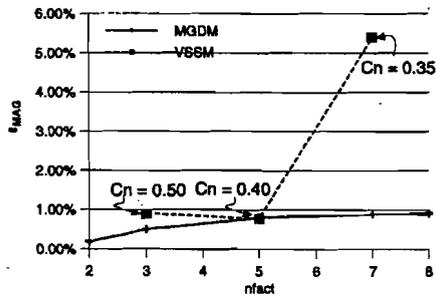

Figure 4: Comparison between phase errors (ϱ_{PHASE}) of the electric field as calculated by MGDM and VSSM. The size of the regions were $4 \times 4 \times 4$ fine grid cells (left) and $8 \times 8 \times 8$ fine grid cells (right). Courant number of 0.57 was used in MGDM (from [16]).
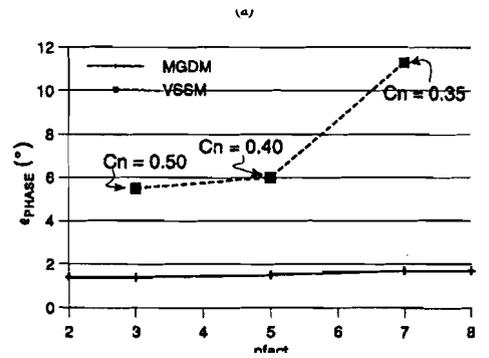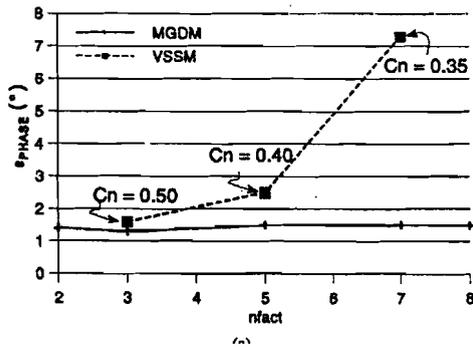
7

To compare VSSM and their own algorithm, called Multigrid Displacement Method (MGDM), White et al. considered a model problem. A waveguide operating at 9.26 GHz is excited by a $TE_1 0$ mode. For the simulations, a cell size of 2.16 mm was chosen. This corresponds to a cell size of 15 per cells per wavelength. Model dimensions (in coarse grid cells) were 42 × 22 × 60. Two different fine-grid grid regions were considered. Dimensions of the first one are 4 × 4 × 4 fine grid cells; dimensions of the second one are 8 × 8 × 8 fine grid cells. These two areas were simulated for the refinement factor $nfact = 2, 3, 4, 5, 7, 8$. Errors are estimated according to the following relations: amplitude errors estimate

$$\varrho_{\text{MAG}} = \left| \frac{E_{\text{uniform}} - E}{E_{\text{uniform}}} \right| \times 100\%,$$

where E_{uniform} is an amplitude of the fields computed on a uniform fine mesh, and phase errors estimate

$$\varrho_{\text{PHASE}} = \left| \frac{\Delta t}{T} \right| \times 180°,$$

where Δt is a difference in zero crossings of the multigrid and the fine grid fields, and T is the period of the sinusoidal excitation.

Comparisons between the amplitude errors are shown in Fig. 3, while the phase errors are shown in Fig. 4. From both figures we can see that the results of the computations for VSSM and MGDM methods are comparable. However, VSSM appears to be less stable, since to maintain stability of VSSM the Courant number (C_n) needs to be decreased as the refinement factor increases. The higher Courant number for MGDM significantly reduces the computational time compared to that of VSSM.

2   Traversing dielectric boundaries

Works of Zivanovic et al. [21], Prescott et al. [12] and White et al. [16] layed a solid foundation for the development of subgridding methods. However, an important issue unresolved in these papers is a dielectric boundary crossing the fine-coarse grid interface. The only way to model two different material areas by the methods described is to make the fine-grid area big enough to contain a single material. However, this is not feasible is the size of either of dielectrics is large, since including the whole dielectric into the fine grid would lead to a significant increase of the computational effort.

In this section we consider two different methods that allow the dielectric boundary to cross the fine-coarse grids interface. The first paper on this subject was
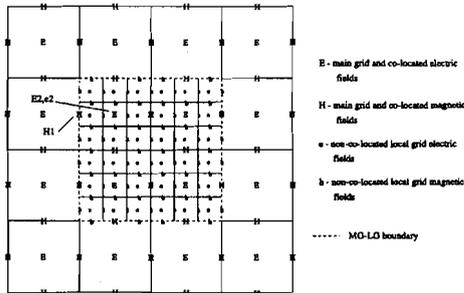
Figure 5: Two-dimensional slice of coarse (main) and fine (local) grids (from [2])

written by Chevalier, Luebbers and Cable in 1997, [2]. The method presented there requires the refinement factor to be an odd number. For simplicity, we consider the refinement factor 3. The approach used in the method is to couple grids by using the tangential magnetic fields on the interface, see fig. 5. The magnetic fields, both tangential and normal are continuous over the interface. Thus a discretisation scheme is simplified for this situation.

First, we consider the collocated magnetic fields on the interface. Assume that fields H^n and $E^{n-1/2}$ to be known. After one step of the FDTD algorithm we know H^{n+1} and $E^{n+1/2}$. Now, using quadratic interpolation we can find the values of h fields for all coarse boundary nodes

$$H^{n+l} = H^n + Al + \frac{Bl^2}{2}, \tag{7}$$

where l is local-grid time increment (1/3, 2/3 or 1) and

$$A = \frac{H^{n+1} - H^{n-1}}{2}, \quad B = H^{n+1} + H^{n-1} - 2H^n.$$

For the rest of the local-grid boundary values, we use linear interpolation. As it turns out from numerical experiments, there exists an instability apparently caused by the difference between the method of obtaining the boundary values and the method (FDTD) of obtaining internal values. Consider a small piece of the composite grid shown in Fig. 6. The field H_1 belongs to the coarse grid and can be computed via FDTD algorithm for the coarse grid. At the same time the neighbouring field h_2 is computed by FDTD on the fine grid. There exists a discontinuity between $H1$ and h_2. This discontinuity can be decreased by weighing h_2 linearly with the neighbouring fields

$$h_2 := 0.95h_2 + 0.05\frac{H_1 + h_3}{2}. \tag{8}$$

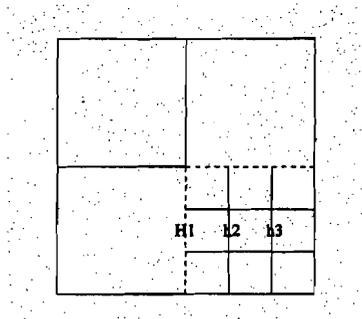The weights (0.95 and 0.05) were determined by numerical experiments.

Figure 6: Magnetic field near the interface (from [2])

Another difficulty lays in oscillations due to low frequency field components being reflected by the interface. This can be suppressed by using a similar weighing approach. Field E_2, see Fig. 5 is a coarse grid field, computed by FDTD on a coarse grid. At the same time the same field happens to be a fine-grid field, and can be computed from FDTD on the fine grid. The new values for E_2 and e_2 are computed as:

$$E_2 := 0.8E_2 + 0.2e_2, \quad e_2 := 0.2E_2 + 0.8e_2. \tag{9}$$

We can thus summarise the algorithm from [2] in the following way:

1. Apply FDTD equations to all main-grid field location (including those inside the local grid) to obtain $E^{n+1/2}$ and H^{n+1}.

2. Apply FDTD equations to all local filed locations for two local-grid time-steps to obtain $e^{n+3/6}$ and $h^{n+4/6}$. Use (7) to obtain h fields at the interface and (8) to obtain h fields one grid cell into the local grid.

3. Apply (9) to weight $E^{n+1/2}$ for the collocated main-grid electric fields closest to the interface and to adjust the collocated $e^{n+3/6}$ field values just obtained.

4. Apply FDTD equations to all local-grid locations for one local time step to obtain $e^{n+5/6}$ and h^{n+1}. Use (7) to obtain interface h fields at the interface and (8) to obtain h fields one cell into the local grid.

5. Transfer all fine-grid h fields which are also coarse-grid fields to the coarse grid.

6. Increase n; return to step 1.

An alternative method to the one of Chevalier, Luebbers and Cable was formulated by White, Yun and Iskander, [17]. The method, called Multigrid Current

10
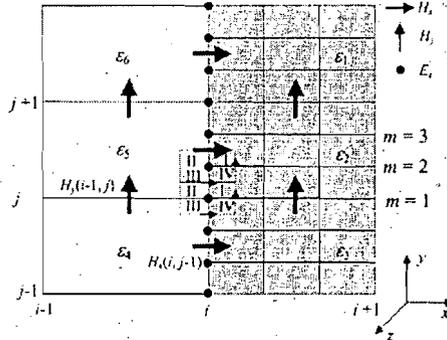
Figure 7: Coarse-fine grid interface, refinement factor (n_{fact}) is three (from [17]).

Method (MGCM) is an update of the Multigrid Displacement Method (MGDM), [16]. The difference between MGCM and MGDM lays in the way of computing the tangential boundary values for the local grid. As we recall, MGDM employed a discrete wave equation at the boundary. MGCM, in turn uses the integral formulation of the Ampere's law

$$\oint \mathbf{H}_C \cdot d\Gamma = \int_S \sigma \mathbf{E} \cdot dS + \frac{d}{dt} \int_S \epsilon \mathbf{E} \cdot dS. \qquad (10)$$

In Fig. 7 we sketch a coarse-fine grid boundary. Arrows denote the magnetic field locations, while dots denote the electric field locations. Various values of ϵ indicate potentially different media.

Let us now briefly review how (10) is used to obtain the boundary values of the electric field. The left-hand side of (10), can be discretised as

$$I_{T_c} \doteq \oint_c \mathbf{H} \cdot d\Gamma = [H_{x,i,j-1} + H_{y,i,j} - H_{x,i,j} - H_{y,i-1,j}]\Delta x_c. \qquad (11)$$

The right-hand side of (10) can be calculated the contribution of each media

11

type to the integral

$$\int_s \sigma \mathbf{E} \cdot dS + \frac{d}{dt} \int_s \epsilon \mathbf{E} \cdot dS$$

$$= \int_S (\sigma_2 E_z + \frac{d}{dt}\epsilon_2 E_z)dS_2$$

$$+ \int_S (\sigma_3 E_z + \frac{d}{dt}\epsilon_3 E_z)dS_3 \qquad (12)$$

$$+ \int_S (\sigma_4 E_z + \frac{d}{dt}\epsilon_4 E_z)dS_4$$

$$+ \int_S (\sigma_5 E_z + \frac{d}{dt}\epsilon_5 E_z)dS_5.$$

The total current can thus be split into parts according to different dielectrics

$$I_{T_c} = I_2 + I_3 + I_4 + I_5, \qquad (13)$$

where e.g.

$$I_2 = [(1 + \overline{\sigma_2})E_z^{n+1} - (1 - \overline{\sigma_2})E_z^n]\frac{\epsilon_0 \epsilon_{r,2}(\Delta x_c)^2}{4\Delta t_c}^2 \;, \quad \overline{\sigma_2} = \frac{\sigma_2 \Delta t_c}{2\epsilon_0 \epsilon_{r,2}}. \qquad (14)$$

Subscript c - means 'coarse'.

The electric field update can now be calculated from

$$E_z^{n+1} = \frac{1 - \overline{\sigma_2}}{1 + \overline{\sigma_2}} E_z^n + \frac{C_n \eta_0}{\overline{\epsilon_0}(1 + \overline{\sigma_c})} \frac{I_{T_c}}{\Delta x_c}, \quad \overline{\sigma_c} = \frac{\overline{\sigma}\Delta t}{2\overline{\epsilon_r}\epsilon_0}, \quad C_n = \frac{c\Delta t_c}{\Delta x_c}, \qquad (15)$$

where I_{T_c} can be found from (11). Similar update equation can be found for the fine grid points at the interface. The problem, however, is that the current passing through the fine cell T_f are unknown. We can treat this current as a sum of currents passing through the quarters of the local cell.

$$I_{T_f} = I_I + I_{II} + I_{III} + I_{IV}. \qquad (16)$$

We assume now that each of the currents is a fixed part of the current passing through the quarter of the global-grid cell

$$I_{T_f} = I_I + I_{II} + I_{III} + I_{IV} = (I_2 + I_5 + I_4 + I_3)\frac{\Delta x_f^2}{\Delta x_c^2} = \frac{I_{T_c}}{n_{\text{fact}}^2}. \qquad (17)$$

3   Combining different coordinate systems

In the previous sections we considered subgridding algorithm where both global domain and local subdomain are of rectangular shape. There are, however problems, where it is more natural to take a ring, or cylinder as a local subdomain.
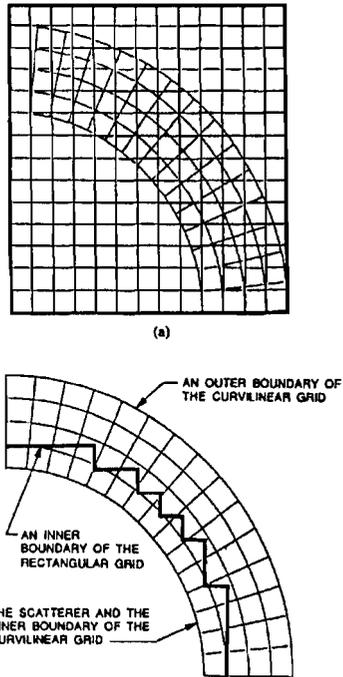
Figure 8: Combination of the cartesian and the curvilinear grid (top), inner boundary of the rectangular grid (bottom) (from [19]).

Such problems occur e.g when modelling a scatterer, which has a cylindrical shape. One of the first algorithms designed to resolve problems involving different coordinate systems was suggested by Yee, Chen and Chang in [19]. The method can be summarised in the following scheme:

1. Choose an appropriate Δx

2. Let S be the scattering surface.
   Denote by
   S_l - the surface consisting of all points at a distance $l\Delta x$ away from S along the exterior pointing normal.
   In the volume enclosed by S and S_3 introduce a conformal grid, see Fig. 8.

3. Introduce a rectangular grid of size Δx. Let V be a union of all FDTD cubes whose centers are at least $1.25\Delta x$ from S. In this case, none of the cubes will intersect S. The inner boundary of V will be the inner boundary of our rectangular grid.

13

4. Interpolate for the tangential electric field at the inner boundary of the rectangular grid from the values at the inner curvilinear boundary.

5. Calculate the magnetic filed on the rectangular grid with the FDTD algorithm.

6. For the curvilinear magnetic field components use an average between the fields calculated on the curvilinear grid and interpolated from the rectangular grid.

7. Interpolate for the outer boundary curvilinear tangential electric field.

Note, that this algorithm is designed to resolve a curvilinear subgrids only, that is the algorithm is not used for refinement.

Another hybrid coordinate system algorithm was suggested by Zhou and Wang in [20].

1. Choose a suitable cylindrical region inside the computational domain, $\Delta\phi$, Δr (for example $\Delta r = \Delta x$). When choosing $\Delta\phi$, let the rectangular and the cylindrical region have as many common point as possible.

2. Choose a suitable inner boundary of the rectangular grid, and let the rectangular grid have at least two-layer overlap with the cylindrical region.

3. The tangential electric field in the outer boundary of the cylindrical grid is obtained through linear interpolation from the values on the rectangular grid. The tangential electric field values in the inner boundary on the rectangular grid are obtained by interpolation from the curvilinear grid.

4. The electric fields at the common points in the overlapping region are obtained by taking an average of the two values.

4 Concluding remarks

In this review we consider a number of subgridding algorithms for FDTD. Despite various differences between the methods described, there is a similar pattern in each of them. So, every author mentioned the fact that certain instabilities occur in subgridding algorithm, most likely due to the discontinuity of the solution across the coarse-fine grid interface. Surprisingly, the same remedy for this instability was proposed in every algorithm: namely to smoothen the solution near the interface by weighing the coarse- and the fine-grid fields. There is, however, no analytical background for such measures.

Among all the algorithms, the algorithm by Chevalier et al. [2] and White et al. [17] seem to the most suitable for the subgridding purposes. They both allow for the dielectric boundaries to cross the coarse-fine grid interface. The algorithm by Chevalier et al. is somewhat simpler, but can work with an odd refinement factor only, while the algorithm by White et al. is more complicated, but allows for an arbitrary refinement. An unfortunate issue is that there is no objective comparison between these two methods.

References

[1] S. Chaillou, J. Wiart, and W. Tabbara. A subgridding scheme based on mesh nesting for the FDTD method. *Microwave and Optical Technology Letters*, 22(3):211–214, August 1999.

[2] Michael W. Chevalier, Raymond J. Luebbers, and Vaughn P. Cable. FDTD local grid with material traverse. *IEEE Transactions on Antennas and Propagation*, 45(3):411–421, March 1997.

[3] M. Feliziani and F. Maradei. Mixed finite-difference/Whitney-elements time domain (FD/WE-TD) method. *IEEE Trasactions on Magnetics*, 34(5):3222–3227, September 1998.

[4] Stavros V. Georgakopoulos, Rosemary A. Renaut, Constantine A. Balanis, and Craig R. Birtcher. A hybrid fourth-order FDTD utilizing a second-order FDTD subgrid. *IEEE Microwave and Wireless Components Letters*, 11(11):462–464, November 2001.

[5] R. Holland and L. Simpson. Finite difference analysis of emp coupling to thin struts and wires. *IEEE Transactions on Electromagnetic Compatibility*, EMC-23:88–97, May 1981.

[6] Ihn S. Kim and Wolfgang J. R. Hoefer. A local mesh refinement algorithm for the time domain–finite difference method using maxwell's curl equations. *IEEE Transactions on Microwave Theory and Techniques*, 38(6):812–815, June 1990.

[7] H. Klingbeil, K. Beilenhoff, and H. L. Hartnagel. A local mesh refinement algorithm for the FDFD method using a polygonal grid. *IEEE Microwave and Guided Wave Letters*, 60(1):52–54, January 1996.

[8] T. O. Körner and W. Fichtner. Grid interpolation at material boundaries in finite-difference time-domain methods. *Microwave and Optical Technology Letters*, 19(5):368–370, December 1998.

[9] K. S. Kunz and L. Simpson. A technique for increasing the resolution of finite-difference solution of the Maxwell equation. *IEEE Transactions on Electromagnetic Compatibility*, EMC-23:419–422, November 1981.

15

[10] A. Monorchino and R. Mittra. A novel subgridding scheme based on a combination of the finite-element and finite-difference time-domain methods. *IEEE Transactions on Antennas and Propagation*, 46(9):1391–1393, September 1998.

[11] Michal Okoniewski, Ewa Okoniewska, and Maria A. Stuchly. Three-dimensional subgridding algorithm for FDTD. *IEEE Transactions on Antennas and Propagation*, 45(3):422–429, March 1997.

[12] Deane T. Prescott and N. V. Shuley. A method for incorporating different sized cells int the finite-difference time-domain analysis technique. *IEEE Microwave and Guided Wave Letters*, 2(11):434–436, November 1992.

[13] P. Thoma and T. Weiland. A consistent subgridding scheme for the finite difference time domain method. *International Journal of Numerical Modelling: Electronic Networks, Devices and Fields*, 9:359–374, 1996.

[14] Bing-Zhong Wang, Yingjun Wang, Wenhua Yu, and Raj Mittra. A hybrid 2-D ADI-FDTD subgridding scheme for modeling on-chip interconnects. *IEEE Transactions on Advanced Packaging*, 24(4):528–533, November 2001.

[15] Shumin Wang, Fernando L. Teixeira, Robert Lee, and Jin-Fa Lee. Optimization of subgridding schemes for FDTD. *IEEE Microwave and Wireless Components Letters*, 12(6), June 2002.

[16] Mikel J. White, Magdy F. Iskander, and Zhenlong Huang. Development of a multigrid FDTD code for three-dimensional applications. *IEEE Transactions on Antennas and Propagation*, 45(10):1512–1517, October 1997.

[17] Mikel J. White, Zhengqing Yun, and Magdy F. Iskander. A new 3-D FDTD multigrid technique with dielectric traverse capabilities. *IEEE Transactions on Microwave Theory and Techniques*, 49(3):422–430, March 2001.

[18] Kane S. Yee. Numerical solutions of initial boundary value problem involving Maxwell's equations in isotropic media. *IEEE Transactions on Antennas and Propagation*, AP-14:302–307, May 1966.

[19] Kane S. Yee, Jei Shuan Chen, and Albert H. Chang. Conformal finite-difference time-domain (FDTD) with overlapping grids. *IEEE Transactions on Antennas and Propagation*, 40(9):1068–1075, September 1992.

[20] Baixin Zhou and Sicong Wang. A hybrid coordinate scheme for enchancing the finite-difference time-domain method. *Microwave and Optical Technology Letters*, 30(2):114–116, July 2001.

[21] Svetlana S. Zivanovic, Kane S. Yee, and Kenneth K. Mei. A subgridding method for the time-domain finite-difference method to solve maxwell's equations. *IEEE Transactions on Microwave Theory and Techniques*, 39(3):471–479, March 1991.